SIAM J. APPL. MATH.
Vol. 68, No. 2, pp. 437–460

RESTORATION OF COLOR IMAGES BY VECTOR VALUED BV FUNCTIONS AND VARIATIONAL CALCULUS*

MASSIMO FORNASIER† AND RICCARDO MARCH‡

Abstract. We analyze a variational problem for the recovery of vector valued functions and compute its numerical solution. The data of the problem are a small set of complete samples of the vector valued function and some significant incomplete information where the former are missing. The incomplete information is assumed as the result of a distortion, with values in a lower dimensional manifold. For the recovery of the function we minimize a functional which is formed by the discrepancy with respect to the data and total variation regularization constraints. We show the existence of minimizers in the space of vector valued bounded variation functions. For the computation of minimizers we provide a stable and efficient method. First, we approximate the functional by coercive functionals on $W^{1,2}$ in terms of Γ-convergence. Then we realize approximations of minimizers of the latter functionals by an iterative procedure to solve the PDE system of the corresponding Euler–Lagrange equations. The numerical implementation comes naturally by finite element discretization. We apply the algorithm to the restoration of color images from limited color information and gray levels where the colors are missing. The numerical experiments show that this scheme is very fast and robust. The reconstruction capabilities of the model are shown, also from very limited (randomly distributed) color data. Several examples are included from the real restoration problem of A. Mantegna's art frescoes in Italy.

Key words. color image processing, systems of partial differential equations, calculus of variations, finite element method

AMS subject classifications. 65M60, 94A08, 49M30, 49J45

DOI. 10.1137/060671875

1. Introduction and examples.

This paper concerns the analysis and the numerical implementation of a variational model for the restoration of vector valued functions. The restoration is obtained from few and sparse *complete* samples of the function and from significant *incomplete* information. The latter is assumed as the result of a nonlinear distortion and with values in a lower dimensional manifold. The applications we consider are in the field of digital signal and image restoration. Therefore, we deal with functional analysis in the space of bounded variation (BV) functions, which are actually considered a reasonable functional model for natural images and signals, usually characterized by discontinuities and piecewise smooth behavior. While in the literature on mathematical image processing mainly real valued BV functions and associated variational problems are discussed (see, for example, [7, 31]), in this contribution we consider vector valued functions.

Since the work of Mumford and Shah [29] and Rudin, Osher, and Fatemi [30], variational calculus techniques have been applied in several image processing problems. We refer the reader to the introductory book [6] for a presentation of this field, more details, and an extended literature.

*Received by the editors October 9, 2006; accepted for publication (in revised form) July 6, 2007; published electronically November 28, 2007.

http://www.siam.org/journals/siap/68-2/67187.html

†Program in Applied and Computational Mathematics, Princeton University, Fine Hall, Washington Road, Princeton, NJ 08544-1000 (mfornasi@math.princeton.edu). This author's work was supported by the European Union's Human Potential Programme under contract MOIF-CT-2006-039438.

‡Consiglio Nazionale delle Ricerche, Istituto per le Applicazioni del Calcolo (IAC) "Mauro Picone," Viale del Policlinico 137, 00161 Roma, Italy (r.march@iac.cnr.it).

FIG. 1.1. *Fragments of A. Mantegna's frescoes* (1452)*, destroyed by a bombing in the Second World War. Computer based reconstruction by using efficient pattern matching techniques* [24] *is shown.*

Inspired by the fresco problem shown in Figure 1.1, a variational model has been proposed by one of the authors in [21]. The problem consists in recovering color in A. Mantegna's frescoes, which were partially destroyed by a bombing in the Second World War. Pieces of the frescoes with the original colors remain, while black and white photos, taken before the war, of the full frescoes are available. Unfortunately, the surface covered by the original fragments is only 77 m^2, while the original area was of several hundreds. This means that what we can currently reconstruct is just a *fraction* (estimated up to 8%) of what this inestimable artwork was. In particular, for most of the frescoes, the *original color* of the blanks is not known. So, natural questions arise: Is it possible to estimate *mathematically* the original colors of the frescoes by using the known fragments' information and the gray level of the pictures taken before the damage? And, how *faithful* is this estimation?

We now introduce some notations. Let Ω be an open, bounded, and connected subset of $\mathbb{R}^N$, and $D \subset \Omega$. The fresco problem is modeled as the reconstruction/restoration of a vector valued function $u : \Omega \to \mathbb{R}^M$ from a given observed couple of functions $(\bar{u}, \bar{v})$. The observed function $\bar{u}$ is assumed to represent correct information on $\Omega \backslash D$, and $\bar{v}$ is the result of a *nonlinear distortion* $\mathcal{L} : \mathbb{R}^M \to \mathbb{R}$ on D.

In particular, a digital image can be modeled as a function $u : \Omega \subset \mathbb{R}^2 \to \mathbb{R}^3_+$, so that, with each "point" $\mathbf{x}$ of the image, one associates the vector $u(\mathbf{x}) = (r(\mathbf{x}), g(\mathbf{x}), b(\mathbf{x})) \in \mathbb{R}^3_+$ of the color represented by the different channels: red, green, and blue. In particular, a digitalization of the image u corresponds to its sampling on a regular lattice $\tau\mathbb{Z}^2$, $\tau > 0$. Let us again write $u : \mathcal{N} \to \mathbb{R}^3_+$, $u(\mathbf{x}) = (r(\mathbf{x}), g(\mathbf{x}), b(\mathbf{x}))$ for $\mathbf{x} \in \mathcal{N} := \Omega \cap \tau\mathbb{Z}^2$.

Usually the gray level of an image can be described as a submanifold $\mathcal{M} \subset \mathbb{R}^3$ by

$$\mathcal{M} := \mathcal{M}_\sigma = \{\sigma(x) : x = \mathcal{L}(r, g, b) := L(\alpha r + \beta g + \gamma b),\ (r, g, b) \in \mathbb{R}^3_+\},$$

where $\alpha, \beta, \gamma > 0$, $\alpha + \beta + \gamma = 1$, $L : \mathbb{R} \to \mathbb{R}$ is a nonnegative increasing function, and $\sigma : \mathbb{R}_+ \to \mathbb{R}^3_+$ is a suitable section such that $\mathcal{L} \circ \sigma = \mathrm{id}_{\mathbb{R}_+}$. The function L is assumed smooth, nonlinear, and normally nonconvex and nonconcave. For example, Figure 1.2 describes the typical shape of an L function, which is estimated by fitting

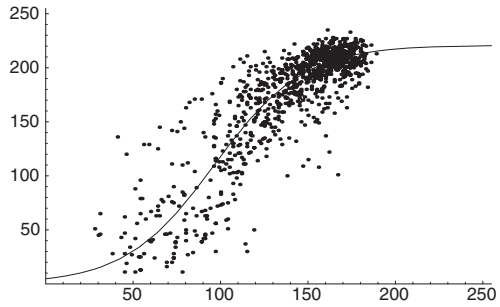

FIG. 1.2. *Estimate of the nonlinear curve L from a distribution of points with coordinates given by the linear combination $\alpha r + \beta g + \gamma b$ of the (red, green, blue) color fragments (abscissa) and by the corresponding underlying gray level of the original photographs dated to* 1920 *(ordinate). The sensitivity parameters α, β, γ to the different frequencies of red, green, and blue are chosen in order to minimize the total variance of the ordinates.*

a distribution of data from the real color fragments in Figure 1.1.

The variational problem proposed in [21] is the following:

$$\arg \inf_{u:\Omega\to\mathbb{R}^M} \left\{ F(u) = \mu \int_{\Omega\setminus D} |u(x) - \bar{u}(x)|^p dx + \lambda \int_D |\mathcal{L}(u(x)) - \bar{v}(x)|^p dx \right. \\ \left. + \int_\Omega \sum_{i=1}^M \phi(|\nabla u_i(x)|) dx \right\}, \tag{1.1}$$

where $p \geq 1$. For example, Figure 1.1 illustrates a typical situation where this model applies. In fact, in this case, there is an area $\Omega\setminus D$ of the domain $\Omega \subset \mathbb{R}^2$ of the image, where some fragments with colors are placed and complete information is available, and another area D (which we call the *inpainting region*), where only the gray-level information is known, modeled as the image of $\mathcal{L}$. The solution of the variational problem (1.1) produces in this case a new color image that extends the colors of the fragments in the gray region. Once the extended color image is transformed by means of $\mathcal{L}$, it is constrained to match the known gray level. We can consider this problem as a generalization of the well-known *image inpainting/disocclusion*; see, e.g., [3, 8, 9, 13, 14, 15, 16]. Several heuristic algorithms have been introduced for colorization of gray images; we refer the reader to the recently appeared paper [33] for related literature and to [26] for numerical examples. Nevertheless, our approach is theoretically founded, more general, and fits with many possible applications, for example, the recovery of a transmitted multichannel signal affected by a stationary (nonlinear) distortion.

For $N = p = 2$, we can compute the Euler–Lagrange equations associated with the functional F and obtain

$$0 = -\nabla \cdot \left(\frac{\phi'(|\nabla u_i|)}{|\nabla u_i|} \nabla u_i \right) \\ + 2\mu(u_i - \bar{u}_i) 1_{\Omega\setminus D} + 2\lambda(\mathcal{L}(u) - \bar{v}) \frac{\partial \mathcal{L}}{\partial u_i}(u) 1_D := \mathcal{E}_i(\mathcal{L}, u), \tag{1.2}$$

$i = 1, \ldots, M$, where $u = (u_1, \ldots, u_M)$ are the components of the function u. This is a system of coupled second order equations, and the analysis of the solutions itself

constitutes a problem of independent interest. By using (1.2) and a finite difference approximation, a steepest-descent algorithm can be formulated as in [21].

Encouraged by the numerical evidence in [21], we discuss the existence of minimizers of the functional F in the context of vector valued BV functions. Our second goal is the formulation of efficient and stable algorithms for the computation of minimizers. Although the steepest-descent scheme recalled above gives appreciable results, it lacks a rigorous analysis and its convergence is usually very slow. For these reasons, we introduce new coercive functionals F_h on $W^{1,2}$ which approximate $\bar{F}$ (the relaxed functional of F with respect to the BV weak-$*$-topology) in terms of Γ-convergence. The computation of minimizers of F_h is performed by an iterative *double-minimization* algorithm; see also [12]. The reconstruction performances are very good, also from very limited (randomly distributed) color data. The virtues of our scheme can be summarized as follows.

1. It is derived as the minimization of a functional and its mathematical analysis and foundations are well described.
2. It implements a total variation (TV) minimization. It is well known [14, 15] that total variation inpainting is affected by two major drawbacks. The first one is that the TV model is only a linear interpolant; i.e., the broken isophotes are interpolated by straight lines. Thus it can generate corners along the inpainting boundary. The second one is that TV often fails to connect widely separated parts of a whole object, due to the high cost in TV measure of making long-distance connections. Due to the constraint on the gray level in the inpainting region, our scheme does not extend isophotes as straight lines and does not violate the *connectivity principle*.
3. As pointed out in [11, 23], while it is relatively easy to recover at higher resolution image portions with relatively uniform color, it might be difficult to recover jumps correctly. Not only should we preserve the morphology and enhance the detail of the discontinuities, but these properties must fit through the different color channels. An incorrect or uncoupled recovery in fact produces "rainbow effects" around jumps. In our functional, the constraint on the gray level in the inpainting region is formulated as a coupled combination of the color channels. In practice, this is sufficient to enforce the correct coupling of the channels at edges.
4. The numerical implementation of our double-minimization scheme is very simple. Its approximation by finite elements comes in a natural way. The scheme is fast and stable.

The paper is organized as follows. In section 2 we introduce the mathematical setting. We recall the main properties of BV functions and a definition of the space of BV functions with vector values. Section 3 is dedicated to results on convex functions and relaxed functionals of measures. In section 4 we collect the assumptions on the nonlinear function $\mathcal{L}$ we will need in our analysis. In section 5 the representation of the relaxed functional $\bar{F}$ of F with respect to the BV topology is given, and the existence and uniqueness of minimizers of $\bar{F}$ are discussed. In section 6 we introduce coercive functionals F_h on $W^{1,2}$ which are shown to Γ-converge to the relaxed functional described above. The double-minimization algorithm to compute minimizers of F_h is illustrated in section 7. Its numerical implementation is presented in section 8. We include several numerical experiments and discuss their results.

2. Vector valued BV functions. In this section we want to introduce notations and preliminary results concerning vector valued BV functions.

We denote by $\mathcal{L}_N$ (and in the integrals dx) the Lebesgue N-dimensional measure in $\mathbb{R}^N$ and by $\mathcal{H}_\alpha$ the α-dimensional Hausdorff measure. Let Ω be an open, bounded, and connected subset of $\mathbb{R}^N$. With $\mathcal{B}(\Omega)$ we denote the family of Borel subsets of $\Omega \subset \mathbb{R}^N$. For a given vector valued measure $\mu : \mathcal{B}(\Omega) \to \mathbb{R}^M$, we denote by $|\mu|$ its total variation, i.e., the finite positive measure

$$|\mu|(A) := \sup\left\{\sum_{j=1}^{M}\int_\Omega v_j d\mu_j : v = (v_1,\dots,v_M) \in C_0(A;\mathbb{R}^M),\ \|v\|_\infty \le 1\right\},$$

for every open set $A \subset \Omega$, where $C_0(A;\mathbb{R}^M) := \overline{C_c(A;\mathbb{R}^M)}^{\|\cdot\|_\infty}$, i.e., the sup-norm closure of the space of continuous function with compact support in A and vector values in $\mathbb{R}^M$. The set of the signed measures on Ω with bounded total variation is denoted by $\mathcal{M}(\Omega)$, coinciding in fact with the topological dual of $(C_0(A;\mathbb{R}^M), \|\cdot\|_\infty)$. Thus, the usual weak-$*$-topology on $\mathcal{M}(\Omega)$ is the weakest topology that makes the maps $\mu \to \int_\Omega f d\mu$ continuous for every continuous function $f \in C_0(A;\mathbb{R}^M)$. In the following we will make use of the notations $x \wedge y := \inf\{x,y\}$ and $x \vee y := \sup\{x,y\}$ for all $x, y \in \mathbb{R}$.

We say that $u \in L^1(\Omega)$ is a real function of bounded variation if its distributional derivative $Du = (D_{x_1}u,\dots,D_{x_N}u)$ is in $\mathcal{M}(\Omega)$. Then the space of bounded variation functions is denoted by

$$BV(\Omega) := \{u \in L^1(\Omega) : Du \in \mathcal{M}(\Omega)\}$$

and, endowed with the norm $\|u\|_{BV(\Omega)} := \|u\|_1 + |Du|(\Omega)$, is a Banach space [20]. More generally, we are interested in vector valued functions with bounded variation components, whose space is defined by

$$BV(\Omega;\mathbb{R}^M) := \{u = (u_1,\dots,u_M) \in L^1(\Omega;\mathbb{R}^M) : u_i \in BV(\Omega)\}.$$

To this space it will turn out to be convenient to attach the norm $\|u\|_{BV(\Omega;\mathbb{R}^M)} := \|u\|_{L^1(\Omega;\mathbb{R}^M)} + \sum_{i=1}^M |Du_i|(\Omega)$. With a slight abuse of notation, for $u \in BV(\Omega;\mathbb{R}^M)$ we denote

$$|Du| := \sum_{i=1}^{M} |Du_i|, \tag{2.1}$$

which again is a finite positive measure for Ω. The space $(BV(\Omega;\mathbb{R}^M), \|\cdot\|_{BV(\Omega;\mathbb{R}^M)})$ is a Banach space. Of course $BV(\Omega;\mathbb{R}^M) = BV(\Omega)$ for $M = 1$, and our notations are consistent with this case.

The product topology of the strong topology of $L^1(\Omega;\mathbb{R}^M)$ for u and of the weak-$*$-topology of measures for Du_i (for all $i = 1,\dots,M$) will be called the weak-$*$-topology of $BV(\Omega;\mathbb{R}^M)$ or the componentwise BV weak-$*$-topology. In the following, whenever the domain Ω and the dimension M will be clearly understood, we will write L^1 instead of $L^1(\Omega;\mathbb{R}^M)$ and BV instead of $BV(\Omega;\mathbb{R}^M)$.

We further recall the main structure properties of BV functions [1, 2, 20]. If $v \in BV(\Omega)$, then the Lebesgue decomposition of Dv with respect to the Lebesgue measure $\mathcal{L}_N$ is given by

$$Dv = \nabla v \cdot \mathcal{L}_N + D_s v,$$

where $\nabla u = \frac{d(Dv)}{dx} \in L^1(\Omega;\mathbb{R}^N)$ is the Radon–Nikodym derivative of Dv and $D_s v$ is singular with respect to $\mathcal{L}_N$.

For a function $v \in L^1(\Omega)$ one denotes by S_v the complement of the Lebesgue set of v, i.e.,

$$S_v := \{x \in \Omega : v^-(x) < v^+(x)\},$$

where

$$v^+(x) := \inf\left\{t \in \bar{\mathbb{R}} : \lim_{\epsilon\to 0} \frac{\mathcal{L}_N(\{v > t\} \cap B(x,\epsilon))}{\epsilon^N} = 0\right\}$$

and

$$v^-(x) := \sup\left\{t \in \bar{\mathbb{R}} : \lim_{\epsilon\to 0} \frac{\mathcal{L}_N(\{v < t\} \cap B(x,\epsilon))}{\epsilon^N} = 0\right\}.$$

Then S_v is countably rectifiable, and for $\mathcal{H}_{N-1}$-a.e. $x \in \Omega$ we can define the outer normal $\nu(x)$. We denote by $\tilde{v} : \Omega \setminus S_v \to \mathbb{R}$ the approximate limit of v defined as $\tilde{v}(x) = v^+(x) = v^-(x)$.

Following [1, 20] $D_s v$ can be expressed by $D_s v = C_v + J_v$, where $J_v = (v^+ - v^-)\nu \cdot \mathcal{H}_{N-1}|_{S_v}$ is the *jump part* and C_v is the *Cantor part* of Dv. Therefore, we can express the measure Dv by

$$Dv = \nabla v \cdot \mathcal{L}_N + C_v + (v^+ - v^-)\nu \cdot \mathcal{H}_{N-1}|_{S_v}, \tag{2.2}$$

and its total variation by

$$|Dv|(E) = \int_E |\nabla v| dx + \int_{E\setminus S_v} |C_v| + \int_{E\cap S_v} (v^+ - v^-) d\mathcal{H}_{N-1}, \tag{2.3}$$

for every Borel set E in the Borel σ-algebra $\mathcal{B}(\Omega)$ of Ω. For major details we refer the reader to [1]. By these properties of real BV functions, one obtains the following result for vector valued BV functions.

LEMMA 2.1 (Lebesgue decomposition for vector valued BV functions). *For $u \in BV(\Omega;\mathbb{R}^N)$, the positive measure $|Du|$ as defined in* (2.1) *has the following Lebesgue decomposition:*

$$|Du| = |D_a u| + |D_s u|, \tag{2.4}$$

where $|D_a u| = \sum_{i=1}^M |\nabla u_i|\mathcal{L}_N$ is the absolutely continuous part and $|D_s u| = \sum_{i=1}^M |C_{u_i}| + \sum_{i=1}^M (u_i^+ - u_i^-)\mathcal{H}_{N-1}|_{S_{u_i}}$ is the singular part of $|Du|$ with respect to the Lebesgue measure $\mathcal{L}_N$.

Proof. By definition it is $|Du| = \sum_{i=1}^M |Du_i|$ and by the Lebesgue decomposition (2.3) for each $|Du_i|$ it is $|Du| = \sum_{i=1}^M \left(|\nabla u_i|\mathcal{L}_N + |C_{u_i}| + (u_i^+ - u_i^-)\mathcal{H}_{N-1}|_{S_{u_i}}\right)$. Since $\sum_{i=1}^M |\nabla u_i|\mathcal{L}_N$ is absolutely continuous and $\sum_{i=1}^M |C_{u_i}| + \sum_{i=1}^M (u^+ - u^-)\mathcal{H}_{N-1}|_{S_{u_i}}$ is singular with respect to $\mathcal{L}_N$, one concludes the proof by the uniqueness of the Lebesgue decomposition. ∎

3. Convex functions and functionals of measures. In the following and throughout the paper we assume that

(A) $\phi : \mathbb{R} \to \mathbb{R}_+$ is an even and convex function, nondecreasing in $\mathbb{R}_+$, such that the following hold:

(i) $\phi(0) = 0$;
(ii) there exist $c > 0$ and $b \geq 0$ such that $cz - b \leq \phi(z) \leq cz + b$ for all $z \in \mathbb{R}$.

Under such conditions the asymptotic recession function ϕ^∞ defined by

$$\phi^\infty(z) := \lim_{y\to\infty} \frac{\phi(yz)}{y}$$

is well defined and bounded. It is $c = \lim_{y\to\infty} \frac{\phi(y)}{y} = \phi^\infty(1)$ and $\phi^\infty(z) = cz \cdot \operatorname{sign}(z)$.

Following [17, 25] we can define convex functions of measures. In particular, if $\mu \in \mathcal{M}(\Omega)$, then we can define

$$\phi(|\mu|) = \phi(|\mu_a|)\mathcal{L}_N + \phi^\infty(1)|\mu_s|,$$

where μ_a and μ_s are the absolutely continuous and singular parts of μ, respectively, with respect to $\mathcal{L}_N$. Therefore, according to Lemma 2.1, if $u \in BV(\Omega;\mathbb{R}^M)$, then

$$\begin{aligned}&\sum_{i=1}^M \phi(|Du_i|)\\ &\quad = \sum_{i=1}^M \phi(|\nabla u_i|)\mathcal{L}_N + \phi^\infty(1)\left(\sum_{i=1}^M |C_{u_i}| + \sum_{i=1}^M (u^+ - u^-)\mathcal{H}_{N-1}|_{S_{u_i}}\right).\end{aligned} \tag{3.1}$$

Definition 3.1. *Let (X,τ) be a topological space satisfying the first axiom of countability and $F : X \to \bar{\mathbb{R}}$. The relaxed functional of F with respect to the topology τ is defined for every $x \in X$ as $\bar{F}(x) := \sup\{G(x) : G$ is τ-lower semicontinuous and $G \leq F\}$. In other words $\bar{F}$ is the maximal τ-lower semicontinuous functional that is smaller than F. We may also write*

$$\bar{F}(u) = \inf_{u^{(n)}\in X,\, u^{(n)} \xrightarrow{\tau} u} \left\{\liminf_n F(u^{(n)})\right\}.$$

We have the following result.

Lemma 3.2. *If $u \in BV(\Omega;\mathbb{R}^M)$ and ϕ is as in assumption* (A)*, then*

$$\begin{aligned}E(u) &:= \int_\Omega \sum_{i=1}^M \phi(|Du_i|) := \sum_{i=1}^M \phi(|Du_i|)(\Omega)\\ &= \int_\Omega \sum_{i=1}^M \phi(|\nabla u_i|)dx + c\left(\sum_{i=1}^M \int_{\Omega\setminus S_{u_i}} |C_{u_i}| + \int_{S_{u_i}} (u_i^+ - u_i^-)d\mathcal{H}_{N-1}\right)\end{aligned}$$

is lower semicontinuous with respect to the componentwise BV weak-$*$-topology.

Proof. It is known that $u_i \to E_i(u_i) := \int_\Omega \phi(|\nabla u_i|)dx + c(\int_{\Omega\setminus S_{u_i}} |C_{u_i}| + \int_{S_{u_i}} (u_i^+ - u_i^-)d\mathcal{H}_{N-1})$ is lower semicontinuous for the BV weak-$*$-topology on $BV(\Omega)$ [25]. One concludes simply by observing that $E(u) = \sum_{i=1}^M E_i(u_i)$. ∎

4. Assumptions on the evaluation map $\mathcal{L}$. In the following we assume that

(L1) $\mathcal{L} : \mathbb{R}^M \to \mathbb{R}_+$ is a nondecreasing continuous function in the sense that $\mathcal{L}(x) \leq \mathcal{L}(y)$ for any $x, y \in \mathbb{R}^M$ such that $|x_i| \leq |y_i|$ for any $i \in \{1,\dots,M\}$;
(L2) $\mathcal{L}(x) \leq a + b|x|^s$ for all $x \in \mathbb{R}^M$ and for fixed $s \geq p^{-1}$, $b > 0$, and $a \geq 0$.

Moreover, one of the two following conditions holds:

(L3-a) $\lim_{x\to\infty} \mathcal{L}(x) = +\infty$;

(L3-b) $\mathcal{L}(x) = \mathcal{L}(x_1, \dots, x_M) = \mathcal{L}((\ell_1 \wedge x_1 \vee -\ell_1), \dots, (\ell_M \wedge x_M \vee -\ell_M))$ for a suitable fixed vector $\ell = (\ell_1, \dots, \ell_M) \in \mathbb{R}^M_+$.

Observe that condition (L3-a) is equivalent to saying that for every $C > 0$ the set $\{\mathcal{L} \leq C\}$ is bounded. Therefore, there exists $A \in \mathbb{R}^M$, with $A_i \geq 0$ for any $i \in \{1, \dots, M\}$, such that $\{\mathcal{L} \leq C\} \subseteq \prod_{i=1}^M [-A_i, A_i]$.

In the following and throughout the paper D denotes a measurable subset of Ω, and we are given the couple $(\bar{u}, \bar{v})$ of bounded functions such that $\bar{u} : \Omega \setminus D \to \mathbb{R}^M$ and $\bar{v} : D \to \mathbb{R}$.

If condition (L3-a) holds, for any measurable function $u : \Omega \to \mathbb{R}^M$, we define the *truncation or clipping operator* as follows:

$$\text{tr}(u, \bar{u}, \Omega, D)(x) := ((\|\bar{u}_i|\Omega \setminus D\|_\infty \vee A_i) \wedge u_i(x) \vee (-\|\bar{u}_i|\Omega \setminus D\|_\infty \wedge -A_i))_{i=1}^M, \tag{4.1}$$

where $A \in \mathbb{R}^M$ is determined so that $\{\mathcal{L} \leq \|\bar{v}|D\|_\infty\} \subseteq \prod_{i=1}^M [-A_i, A_i]$. Analogously we define the truncation operator in the case of condition (L3-b):

$$\text{tr}(u, \bar{u}, \bar{v}, \Omega, D)(x) := ((\|\bar{u}_i|\Omega \setminus D\|_\infty \vee \ell_i) \wedge u_i(x) \vee (-\|\bar{u}_i|\Omega \setminus D\|_\infty \wedge -\ell_i))_{i=1}^M. \tag{4.2}$$

In the case when it is clear which of the conditions (L3-a,b) holds and the set D and the functions $\bar{u}, \bar{v}$ are given, then it will be convenient to use the shorter notation $\hat{u} := \text{tr}(u, \bar{u}, \bar{v}, \Omega, D)$.

For any measurable function $u : \Omega \to \mathbb{R}^M$ we define

$$G_1(u) = \int_{\Omega \setminus D} |u(x) - \bar{u}(x)|^p dx, \tag{4.3}$$

$$G_2(u) = \int_D |\mathcal{L}(u(x)) - \bar{v}(x)|^p dx. \tag{4.4}$$

LEMMA 4.1. *For any $u \in BV(\Omega; \mathbb{R}^M)$ the truncation operator has the property that $\hat{u} \in BV(\Omega; \mathbb{R}^M)$, and*

$$G_i(\hat{u}) \leq G_i(u), \quad i = 1, 2, \quad \text{and } E(\hat{u}) \leq E(u). \tag{4.5}$$

Proof. Let us assume that condition (L3-a) holds. If $x \in \Omega \setminus D$, the definition of the truncation operator implies that $|\hat{u}(x) - \bar{u}(x)| \leq |u(x) - \bar{u}(x)|$, from which it follows that $G_1(\hat{u}) \leq G_1(u)$. If $x \in D$ is such that $u(x) \in \prod_{i=1}^M [-\|\bar{u}_i|\Omega \setminus D\|_\infty \wedge -A_i, \|\bar{u}_i|\Omega \setminus D\|_\infty \vee A_i]$, then $\hat{u}(x) = u(x)$. Otherwise, $x \notin \prod_{i=1}^M [-A_i, A_i]$ and $|u_i(x)| \geq |\hat{u}_i(x)| \geq |\xi_i|$ for any ξ such that $\mathcal{L}(\xi) \leq \|\bar{v}|D\|_\infty$ and any $i \in \{1, \dots, M\}$. Therefore, by the monotonicity assumption (L1) $\mathcal{L}(u(x)) \geq \mathcal{L}(\hat{u}(x)) \geq \|\bar{v}|D\|_\infty$, which implies that $|\mathcal{L}(\hat{u}(x)) - \bar{v}(x)| \leq |\mathcal{L}(u(x)) - \bar{v}(x)|$ for any $x \in D$, and $G_2(\hat{u}) \leq G_2(u)$. The proof is analogous if condition (L3-b) holds.

We now prove the corresponding statement for the functional E. Fix $i \in \{1, \dots, M\}$. By definition of the truncation operator, we have $\hat{u}_i = g_i \circ u_i$, where $g_i : \mathbb{R} \to \mathbb{R}$ is a Lipschitz function such that

$$g_i(t) = \begin{cases} t, & -c_i \leq t \leq d_i, \\ d_i, & t > d_i, \\ -c_i, & t < -c_i, \end{cases}$$

where $c_i, d_i > 0$ are determined by (4.1), (4.2). Using the chain rule for real valued BV functions (Theorem 3.99 of [2]), we have that $\hat{u} \in BV(\Omega; \mathbb{R}^M)$ and

$$D\hat{u}_i = g_i'(u_i)\nabla u_i \cdot \mathcal{L}_N + g_i'(\tilde{u}_i)C_{u_i} + \left(g_i(u_i^+) - g_i(u_i^-)\right)\nu_i \cdot \mathcal{H}_{N-1}|_{S_{u_i}},$$

where $\tilde{u}_i$ is the approximate limit of u_i. Then $\nabla\hat{u}_i(x) = \nabla u_i(x)$ if $-c_i < u_i(x) < d_i$, and $\nabla\hat{u}_i(x) = 0$ if either $u_i(x) > d_i$ or $u_i(x) < -c_i$. Moreover, by Proposition 3.73(c) of [2] it follows that $\nabla u_i(x) = 0$ for a.e. $x \in \{u_i(x) = d_i\}$ and a.e. $x \in \{u_i(x) = -c_i\}$. Hence $|\nabla\hat{u}_i(x)| \le |\nabla u_i(x)|$ a.e., so that from assumption (A) of the function ϕ we get

$$\int_\Omega \phi(|\nabla\hat{u}_i|)dx \le \int_\Omega \phi(|\nabla u_i|)dx. \tag{4.6}$$

Since $u_i^+(x) \ge u_i^-(x)$ for any $x \in S_{u_i}$, by the definition of the function g_i we have

$$S_{\hat{u}_i} \subseteq S_{u_i}, \qquad g_i(u_i^+(x)) - g_i(u_i^-(x)) \le u_i^+(x) - u_i^-(x) \quad \text{for any } x \in S_{u_i}.$$

Then it follows that

$$\int_{S_{\hat{u}_i}} (\hat{u}_i^+ - \hat{u}_i^-)d\mathcal{H}_{N-1} \le \int_{S_{u_i}} (u_i^+ - u_i^-)d\mathcal{H}_{N-1}. \tag{4.7}$$

By the definition of g_i we then have $0 \le g_i'(\tilde{u}_i(x)) \le 1$ for any $x \in \{x : \tilde{u}_i(x) \ne d_i\} \cap \{x : \tilde{u}_i(x) \ne -c_i\}$. Moreover, by Proposition 3.92(c) of [2], the Cantor part C_{u_i} vanishes on sets of the form $\tilde{u}_i^{-1}(Q)$ with $Q \subset \mathbb{R}$, $\mathcal{H}_1(Q) = 0$. It follows that C_{u_i} vanishes on the set $\{x : \tilde{u}_i(x) = d_i\} \cup \{x : \tilde{u}_i(x) = -c_i\}$, so that we get $|C_{\hat{u}_i}|(\Omega) \le |C_{u_i}|(\Omega)$, i.e.,

$$\int_{\Omega\setminus S_{\hat{u}_i}} |C_{\hat{u}_i}| \le \int_{\Omega\setminus S_{u_i}} |C_{u_i}|. \tag{4.8}$$

Collecting the inequalities (4.6)–(4.8) and summing over $i = 1, \dots, M$, we obtain $E(\hat{u}) \le E(u)$, which concludes the proof. □

REMARK 4.2. *The truncation operator maps C_0^1 functions into $W^{1,q}$; i.e., for any $u \in C_0^1(\Omega;\mathbb{R}^M)$ we have* $\mathrm{tr}(u, \bar{u}, \bar{v}, \Omega, D) \in W^{1,q}(\Omega;\mathbb{R}^M)$ *for any* $1 \le q \le \infty$.

5. Relaxation and existence of minimizers. The functional F is well defined in $L^\infty(\Omega;\mathbb{R}^M) \cap W^{1,1}(\Omega;\mathbb{R}^M)$. Since this space is not reflexive, and sequences that are bounded in $W^{1,1}$ are also bounded in BV, we extend F to the space $BV(\Omega;\mathbb{R}^M)$ in such a way that the extended functional is lower semicontinuous. By using the relaxation method of the calculus of variations, the natural candidate for the extended functional is the relaxed functional $\bar{F}$ of F with respect to the componentwise BV weak-$*$-topology [6].

In the following, without loss of generality, we set $\mu = \lambda = 1$.

5.1. Relaxation. We set $X = \{u \in BV(\Omega;\mathbb{R}^M) : \|u_i\|_\infty \le K_i,\ i = 1, \dots, M\}$, where, for any $i \in \{1, \dots, M\}$, the constant $K_i > 0$ is defined by $K_i = \max\{A_i, \|\bar{u}_i|\Omega\setminus D\|_\infty\}$ if condition (L3-a) holds, and by $K_i = \max\{\ell_i, \|\bar{u}_i|\Omega\setminus D\|_\infty\}$ if condition (L3-b) holds.

The following theorem extends to our case the relaxation result proved in [6, Theorem 3.2.1].

THEOREM 5.1. *The relaxed functional of F in X with respect to the componentwise BV weak-$*$-topology is given by*

$$\begin{aligned}\bar{F}(u) = &\int_{\Omega\setminus D} |u(x) - \bar{u}(x)|^p dx + \int_D |\mathcal{L}(u(x)) - \bar{v}(x)|^p dx \\ &+ \int_\Omega \sum_{i=1}^M \phi(|\nabla u_i|)dx + c\left(\sum_{i=1}^M \int_{\Omega\setminus S_{u_i}} |C_{u_i}| + \int_{S_{u_i}} (u_i^+ - u_i^-)d\mathcal{H}_{N-1}\right).\end{aligned}$$

Proof. Let us define

$$f(u) := \begin{cases} F(u), & u \in X \cap W^{1,1}(\Omega;\mathbb{R}^M), \\ +\infty, & u \in X \setminus W^{1,1}(\Omega;\mathbb{R}^M). \end{cases}$$

Observe that $f(u) = \bar{F}(u)$ for $u \in W^{1,1}(\Omega;\mathbb{R}^M)$.

By property (L2) we have that $G_1(u), G_2(u) < +\infty$ for all $u \in X$. By using Fatou's lemma the functionals G_1 and G_2 are lower semicontinuous with respect to the strong L^1 topology and hence with respect to the componentwise BV weak-$*$-topology. Therefore, by Lemma 3.2, $\bar{F}$ is lower semicontinuous in X with respect to such topology.

Let $\bar{f}$ denote the relaxed functional of f in X with respect to the same topology. Since $\bar{F}(u) \le f(u)$ for any $u \in X$, and $\bar{f}$ is the greatest lower semicontinuous functional less than or equal to f, we have $\bar{f}(u) \ge \bar{F}(u)$ for any $u \in X$. Then we have to show that $\bar{f}(u) \le \bar{F}(u)$.

By [17, Theorems 2.2 and 2.3] for any $u \in X$ there exists a sequence $\{u^{(n)}\}_n \subset C_0^\infty(\Omega;\mathbb{R}^M) \cap W^{1,1}(\Omega;\mathbb{R}^M)$ such that $u^{(n)}$ converges to u in the componentwise BV weak-$*$-topology and $E(u) = \lim_n E(u^{(n)})$.

Let us now consider the sequence $\{\hat{u}^{(n)}\}_n$ of the truncated functions. By Lemma 4.1 we have

$$E(u) = \lim_n E(u^{(n)}) \ge \limsup_n E(\hat{u}^{(n)}). \tag{5.1}$$

With similar computations as those in the proof of Lemma 4.1

$$\int_\Omega |\hat{u}^{(n)}(x) - u(x)|dx \le \int_\Omega |u^{(n)}(x) - u(x)|dx \to 0, \quad n \to \infty.$$

Moreover, since the truncated functions $\hat{u}^{(n)}$ are uniformly bounded in $L^\infty(\Omega;\mathbb{R}^M)$, then $\hat{u}^{(n)}$ converges to u in $L^q(\Omega;\mathbb{R}^M)$ for any $1 \le q < \infty$.

Now the functional G_1 is continuous with respect to the strong $L^p(\Omega \setminus D;\mathbb{R}^M)$ topology. Moreover, since $\mathcal{L}$ is continuous, the functional G_2 is continuous with respect to the strong $L^q(D;\mathbb{R}^M)$ topology, with $q = sp \ge 1$ (see [19, Chapter 9, Lemma 3.2]).

Then, using (5.1), the continuity properties of G_1 and G_2, and Remark 4.2, we have $\hat{u}^{(n)} \in W^{1,1}(\Omega;\mathbb{R}^M)$, $\bar{F}(\hat{u}^{(n)}) = f(\hat{u}^{(n)})$, and

$$\begin{aligned} \bar{F}(u) &= G_1(u) + G_2(u) + E(u) \ge \lim_n (G_1(\hat{u}^{(n)}) + G_2(\hat{u}^{(n)})) + \limsup_n E(\hat{u}^{(n)}) \\ &\ge \limsup_n f(\hat{u}^{(n)}) \ge \liminf_n f(\hat{u}^{(n)}) \ge \inf_{u^{(n)} \in BV,\, u^{(n)} \overset{BV-w^*}{\to} u} \left\{ \liminf_n f(u^{(n)}) \right\} = \bar{f}(u). \end{aligned}$$

Then we have $\bar{F}(u) = \bar{f}(u)$ and the statement is proved. ∎

5.2. Existence and uniqueness of minimizers. In this section we shall prove the existence of minimizers of $\bar{F}$ in X and state the conditions for the uniqueness.

THEOREM 5.2. *There exists a solution of the following variational problem:*

$$\min_{u \in X} \left\{ \bar{F}(u) = \int_{\Omega \setminus D} |u(x) - \bar{u}(x)|^p dx + \int_D |\mathcal{L}(u(x)) - \bar{v}(x)|^p dx \right.$$
$$\left. + \int_\Omega \sum_{i=1}^M \phi(|\nabla u_i|)dx + c \left(\sum_{i=1}^M \int_{\Omega \setminus S_{u_i}} |C_{u_i}| + \int_{S_{u_i}} (u_i^+ - u_i^-) d\mathcal{H}_{N-1} \right) \right\}.$$

In particular, we have

$$\min_{u\in X} \bar{F}(u) = \inf_{u\in X} F(u).$$

Moreover, if $D \subsetneq \Omega$ and G_2 is a strictly convex functional, then the solution is unique.

Proof. Let $\{u^{(n)}\}_n$ be a minimizing sequence in BV. By assumption (A)(ii) in section 3, there exists a constant $C > 0$ such that $|Du^{(n)}|(\Omega) \le C$ uniformly with respect to n. By Lemma 4.1 we can modify the minimizing sequence by truncation, obtaining a new minimizing sequence $\{\hat{u}^{(n)}\}_n \subset X$. By Lemma 4.1 this sequence is uniformly bounded in $BV(\Omega;\mathbb{R}^M)$, i.e.,

$$\|\hat{u}^{(n)}\|_\infty \le \max_{i=1,\dots,M} K_i, \qquad |D\hat{u}^{(n)}|(\Omega) \le C$$

for any n. Therefore, there exists a subsequence $\{\hat{u}^{(n_k)}\}_k$ converging with respect to the componentwise BV weak-$*$-topology to a function $u \in X$. Since the relaxed functional $\bar{F}$ is lower semicontinuous in X with respect to such a topology, we have

$$\bar{F}(u) \le \liminf_k \bar{F}(u^{(n_k)}).$$

From the compactness and lower semicontinuity properties of $\bar{F}$ it follows that $u \in X$ is a minimizer of $\bar{F}$. Moreover, if $D \subsetneq \Omega$ and G_2 is a strictly convex functional, then $\bar{F}$ is strictly convex and the solution u is unique. Since F is coercive in X, one concludes by an application of [27, Theorem 3.8]. ∎

6. Approximation by Γ-convergence. In this section we endow the space X with the L^1 strong topology, and we show that minimizers of $\bar{F}$ can be approximated in X by minimum points of functionals that are defined in $W^{1,2}(\Omega;\mathbb{R}^M)$.

For a positive decreasing sequence $\{\varepsilon_h\}_{h\in\mathbb{N}}$ such that $\lim_{h\to\infty} \varepsilon_h = 0$, and for $\phi \in C^1(\mathbb{R})$, we define

$$F_h(u) = \begin{cases} G_1(u) + G_2(u) + \displaystyle\int_\Omega \sum_{i=1}^M \phi_h(|\nabla u_i(x)|)dx, & u \in W^{1,2}(\Omega;\mathbb{R}^M), \\ +\infty, & u \in X \setminus W^{1,2}(\Omega;\mathbb{R}^M), \end{cases} \tag{6.1}$$

where

$$\phi_h(z) = \begin{cases} \dfrac{\phi'(\varepsilon_h)}{2\varepsilon_h} z^2 + \phi(\varepsilon_h) - \dfrac{\varepsilon_h \phi'(\varepsilon_h)}{2}, & 0 \le z \le \varepsilon_h, \\ \phi(z), & \varepsilon_h \le z \le \dfrac{1}{\varepsilon_h}, \\ \dfrac{\varepsilon_h \phi'(1/\varepsilon_h)}{2} z^2 + \phi\left(\dfrac{1}{\varepsilon_h}\right) - \dfrac{\phi'(1/\varepsilon_h)}{2\varepsilon_h}, & z \ge \dfrac{1}{\varepsilon_h}. \end{cases}$$

If $z \mapsto \frac{\phi'(z)}{z}$ is continuously decreasing, then $\phi_h(z) \ge \phi(z) \ge 0$ for any h and any z, and $\lim_h \phi_h(z) = \phi(z)$ for any z.

By means of standard arguments we have that for any h the functional F_h has a minimizer in $X \cap W^{1,2}(\Omega;\mathbb{R}^M)$; see, e.g., [31, Proposition 6.1]. Moreover, if $D \subsetneq \Omega$ and G_2 is a strictly convex functional, then the minimizer is unique. The following theorem extends to our case the Γ-convergence result proved in [31, Proposition 6.1]; see also Theorem 3.2.3 of [6]. We do not introduce the concept of Γ-convergence which

is used here only as an auxiliary tool. We refer the reader to [27] and the relevant results therein for more details, in particular, [27, Proposition 5.7, Theorem 7.8, Corollary 7.20, Corollary 7.24].

THEOREM 6.1. *Let $\{u^{(h)}\}_h$ be a sequence of minimizers of F_h. Then $\{u^{(h)}\}_h$ is relatively compact in $L^1(\Omega;\mathbb{R}^M)$, each of its limit points minimizes the functional $\bar{F}$, and*

$$\min_{u\in X} \bar{F}(u) = \lim_{h\to\infty} \min_{u\in X\cap W^{1,2}} F_h(u).$$

Moreover, if $D \subsetneq \Omega$ and G_2 is a strictly convex functional, we have

$$\lim_{h\to\infty} u^{(h)} = u^{(\infty)} \text{ in } X, \quad \lim_{h\to\infty} F_h(u^{(h)}) = \bar{F}(u^{(\infty)}), \tag{6.2}$$

where $u^{(\infty)}$ is the unique minimizer of $\bar{F}$ in X.

Proof. We define

$$g(u) = \begin{cases} F(u), & u \in X \cap W^{1,2}(\Omega;\mathbb{R}^M), \\ +\infty, & u \in X \setminus W^{1,2}(\Omega;\mathbb{R}^M). \end{cases}$$

Observe that g is the restriction of F to functions $u \in W^{1,2}(\Omega;\mathbb{R}^M)$.

By construction we have that $\{F_h\}_h$ is a decreasing sequence of functionals that converges pointwise to g in $X \cap W^{1,2}(\Omega;\mathbb{R}^M)$. Therefore, by [27, Proposition 5.7], F_h Γ-converges to the relaxed functional $\bar{g}$ of g in X with respect to the $L^1(\Omega;\mathbb{R}^M)$ topology. Then we have to show that $\bar{F} = \bar{g}$.

Let $\{u^{(n)}\}_n \subset X$ be a sequence such that $u^{(n)} \to u$ in $L^1(\Omega;\mathbb{R}^M)$ and $\liminf_n \bar{F}(u^{(n)}) < +\infty$. Up to the extraction of a subsequence we may assume that $\liminf_n \bar{F}(u^{(n)}) = \lim_n \bar{F}(u^{(n)})$. Then $\bar{F}(u^{(n)})$ is uniformly bounded with respect to n, so that $\{u^{(n)}\}_n$ is uniformly bounded in BV. Then, up to a subsequence, $u^{(n)}$ converges to u in the componentwise BV weak-$*$-topology and, by Theorem 5.1, we have $\liminf_n \bar{F}(u^{(n)}) \geq \bar{F}(u)$. Hence $\bar{F}$ is lower semicontinuous in X with respect to the $L^1(\Omega;\mathbb{R}^M)$ topology.

Then, arguing as in the proof of Theorem 5.1, for any function $u \in X$ there exists a sequence of truncated functions $\hat{u}^{(n)} \in W^{1,2}(\Omega;\mathbb{R}^M) \cap X$ such that

$$\hat{u}^{(n)} \to u \text{ in } L^1(\Omega;\mathbb{R}^M) \quad \text{and} \quad \bar{F}(u) \geq \liminf_{n\to\infty} g(\hat{u}^{(n)}). \tag{6.3}$$

Since $g \geq \bar{F}$, property (6.3) implies that $\bar{F} \geq \bar{g}$. Then, by the lower semicontinuity of $\bar{F}$ with respect to the $L^1(\Omega;\mathbb{R}^M)$ topology, we have $\bar{F} = \bar{g}$. Therefore, F_h Γ-converges to $\bar{F}$.

By construction $\phi_h(z) \geq \phi(z)$ for any $z \geq 0$, so that $F_h(u) \geq \bar{F}(u)$ for any h and any $u \in X$. Since $\bar{F}$ is coercive and lower semicontinuous in $L^1(\Omega;\mathbb{R}^M)$, it follows that the sequence $\{F_h\}_h$ is equicoercive in $L^1(\Omega;\mathbb{R}^M)$. In particular, any family $\{u^{(h)}\}_h$ of minimizers of F_h is relatively compact in $L^1(\Omega;\mathbb{R}^M)$. Then, using [27, Theorem 7.8], the limit points of sequences of minimizers of F_h minimize $\bar{F}$ and $\min_{u\in X} \bar{F}(u) = \lim_h \min_{u\in W^{1,2}} F_h(u)$.

Finally, if $D \subsetneq \Omega$ and G_2 is a strictly convex functional, by Theorem 5.2 there exists a unique minimizer of $\bar{F}$ in X. Therefore the limits (6.2) follow from Corollary 7.24 of [27]. ∎

REMARK 6.2. *So far we have considered evaluation maps $\mathcal{L} : \mathbb{R}^M \to \mathbb{R}$. However, the whole analysis can be generalized to the case $\mathcal{L} : \mathbb{R}^M \to \mathcal{M}$, $\mathcal{L}(x) =$*

$(\mathcal{L}_1(x),\dots,\mathcal{L}_D(x))$, where $\mathcal{M}\subset\mathbb{R}^M$ is a $(D\le M)$-dimensional submanifold. However, for $D=1$ and L usually being an invertible map, it is possible to "reequalize" the gray level so that $\mathcal{L}(x)=\frac{1}{M}(x_1+\cdots+x_M)$. Later in this paper, for simplicity purposes in numerical implementation, we will use such linearization for $\mathcal{L}$.

7. Euler–Lagrange equations and a relaxation algorithm. In this section we want to provide an algorithm to compute efficiently minimizers of the approximating functionals F_h. First, we want to derive the Euler–Lagrange equations associated with F_h. In the following we assume that both ϕ_h and $\mathcal{L}$ are continuously differentiable and that Ω is an open, bounded, and connected subset of $\mathbb{R}^N$ with Lipschitz boundary $\partial\Omega$. Moreover, $p=2$ if $N=1$ and $p=\frac{N}{N-1}$ for $N>1$, $1/p+1/p'=1$. By standard arguments we have the following result.

PROPOSITION 7.1. *If u is a minimizer in $W^{1,2}(\Omega;\mathbb{R}^M)$ of F_h, then u solves the following system of Euler–Lagrange equations:*

$$\begin{cases} 0=-\operatorname{div}\left(\frac{\phi_h'(|\nabla u_i|)}{|\nabla u_i|}\nabla u_i\right)+p|u-\bar u|^{p-2}(u_i-\bar u_i)1_{\Omega\setminus D}+p|\mathcal{L}(u)\\ \qquad -\bar v|^{p-2}(\mathcal{L}(u)-\bar v)\frac{\partial\mathcal{L}}{\partial u_i}(u)1_D,\\ \frac{\phi_h'(|\nabla u_i|)}{|\nabla u_i|}\frac{\partial u_i}{\partial\nu}=0 \text{ on } \partial\Omega,\quad i=1,\dots,M. \end{cases}$$

The former equalities hold in the sense of distributions and in $L^{p'}(\Omega;\mathbb{R}^M)$.

The previous equations yield a necessary condition for the computation of minimizers of F_h. Again we are not ensured of the uniqueness in general, unless G_2 is strictly convex. The system is composed of M second order *nonlinear* equations which are coupled on terms of order 0. Both the nonlinear term $\operatorname{div}\left(\frac{\phi_h'(|\nabla u_i|)}{|\nabla u_i|}\nabla u_i\right)$ and the coupled terms of order 0 constitute a complication for the numerical solution of these equations.

Based on the work [12, 18, 32], we propose in the following a method to compute efficiently solutions of the Euler–Lagrange equations, which simplifies the problem of the nonlinearity. Since we want to illustrate concrete applications for color image recovery, for simplicity, we limit our analysis to the case $N=p=2$ and $\phi(t)=|t|$ for all $t\in\mathbb{R}$. Let us introduce a new functional given by

$$\mathcal{E}_h(u,w):=2\,(G_1(u)+G_2(u))+\int_\Omega\sum_{i=1}^M\left(w_i|\nabla u_i(x)|^2+\frac{1}{w_i}\right)dx, \tag{7.1}$$

where $u\in W^{1,2}(\Omega;\mathbb{R}^M)$, and $w\in L^2(\Omega;\mathbb{R}^M)$ is such that $\varepsilon_h\le w_i\le\frac{1}{\varepsilon_h}$, $i=1,\dots,M$. While the variable u again is the function to be reconstructed, we call the variable w the *gradient weight*. In the following, since we assume h fixed, we drop the index h from the functional $\mathcal{E}_h$.

For any given $u^{(0)}\in X\cap W^{1,2}(\Omega;\mathbb{R}^M)$ and $w^{(0)}\in L^2(\Omega;\mathbb{R}^M)$ (for example, $w^{(0)}:=1$), we define the following iterative double-minimization algorithm:

$$\begin{cases} u^{(n+1)}=\arg\min_{u\in W^{1,2}(\Omega;\mathbb{R}^M)}\mathcal{E}(u,w^{(n)}),\\ w^{(n+1)}=\arg\min_{\varepsilon_h\le w\le\frac{1}{\varepsilon_h}}\mathcal{E}(u^{(n+1)},w). \end{cases} \tag{7.2}$$

We have the following convergence result.

THEOREM 7.2. *The sequence $\{u^{(n)}\}_{n\in\mathbb{N}}$ has subsequences that converge strongly in $L^2(\Omega;\mathbb{R}^M)$ and weakly in $W^{1,2}(\Omega;\mathbb{R}^M)$ to a stationary point $u^{(\infty)}$ of F_h; i.e., $u^{(\infty)}$*

solves the Euler–Lagrange equations in Proposition 7.1. *Moreover, if F_h has a unique minimizer u^*, then $u^{(\infty)} = u^*$ and the full sequence $\{u^{(n)}\}_{n\in\mathbb{N}}$ converges to u^*.*

Proof. Observe that

$$\mathcal{E}(u^{(n)}, w^{(n)}) - \mathcal{E}(u^{(n+1)}, w^{(n+1)}) = \underbrace{\left(\mathcal{E}(u^{(n)}, w^{(n)}) - \mathcal{E}(u^{(n+1)}, w^{(n)})\right)}_{A_n} + \underbrace{\left(\mathcal{E}(u^{(n+1)}, w^{(n)}) - \mathcal{E}(u^{(n+1)}, w^{(n+1)})\right)}_{B_n} \geq 0.$$

Therefore, $\mathcal{E}(u^{(n)}, w^{(n)})$ is a nonincreasing sequence and, moreover, it is bounded from below, since

$$\inf_{\varepsilon_h \leq w \leq 1/\varepsilon_h} \int_\Omega \sum_{i=1}^M \left(w_i |\nabla u_i(x)|^2 + \frac{1}{w_i} \right) dx \geq 0.$$

This implies that $\mathcal{E}(u^{(n)}, w^{(n)})$ converges. Moreover, we can write

$$B_n = \int_\Omega \sum_{i=1}^M c(w_i^{(n)}(x), |\nabla u_i^{(n+1)}(x)|) - c(w_i^{(n+1)}(x), |\nabla u_i^{(n+1)}(x)|) dx,$$

where $c(t,z) := tz^2 + \frac{1}{t}$. By Taylor's formula, we have

$$c(w_i^{(n)}, z) = c(w_i^{(n+1)}, z) + \frac{\partial c}{\partial t}(w_i^{(n+1)}, z)(w_i^{(n)} - w_i^{(n+1)}) + \frac{1}{2}\frac{\partial^2 c}{\partial t^2}(\xi, z)|w_i^{(n)} - w_i^{(n+1)}|^2$$

for $\xi \in \mathrm{conv}(w_i^{(n)}, w_i^{(n+1)})$. By definition of $w_i^{(n+1)}$ and taking into account that $\varepsilon_h \leq w_i^{(n+1)} \leq \frac{1}{\varepsilon_h}$, we have

$$\frac{\partial c}{\partial t}(w_i^{(n+1)}, |\nabla u_i^{(n+1)}(x)|)(w_i^{(n)} - w_i^{(n+1)}) \geq 0,$$

and $\frac{\partial^2 c}{\partial t^2}(t,z) = \frac{2}{t^3} \geq 2\varepsilon_h^3$, for any $t \leq 1/\varepsilon_h$. This implies that

$$\mathcal{E}(u^{(n)}, w^{(n)}) - \mathcal{E}(u^{(n+1)}, w^{(n+1)}) \geq B_n \geq \varepsilon_h^3 \int_\Omega \sum_{i=1}^M |w_i^{(n)}(x) - w_i^{(n+1)}(x)|^2 dx,$$

and since $\mathcal{E}(u^{(n)}, w^{(n)})$ is convergent, we have $\sum_{i=1}^M \int_\Omega |w_i^{(n)}(x) - w_i^{(n+1)}(x)|^2 dx \to 0$ for $n \to \infty$. In fact it holds that

$$\|w_i^{(n)} - w_i^{(n+1)}\|_{L^q} \to 0, \quad i = 1, \ldots, M, \tag{7.3}$$

for $n \to \infty$ and for any $1 \leq q < \infty$. Since $u^{(n+1)}$ is a minimizer of $\mathcal{E}(u, w^{(n)})$, it solves the following system of variational equations:

$$\int_\Omega \Big(w_i^{(n)} \nabla u_i^{(n+1)}(x) \cdot \nabla \varphi_i(x) + 2(u_i^{(n+1)}(x) - \bar{u}_i(x)) 1_{\Omega \setminus D}(x) + 2(\mathcal{L}(u^{(n+1)}(x)) - \bar{v}(x)) \frac{\partial \mathcal{L}}{\partial u_i}(u^{(n+1)}(x)) 1_D(x) \Big) \varphi_i(x) dx = 0 \tag{7.4}$$

for $i = 1, \dots, M$ and for all $\varphi \in W^{1,2}(\Omega; \mathbb{R}^M)$. Therefore, we can write

$$\int_\Omega \left(w_i^{(n+1)} \nabla u_i^{(n+1)}(x) \cdot \nabla \varphi_i(x) + 2(u_i^{(n+1)}(x) - \bar{u}_i(x)) 1_{\Omega \setminus D}(x) \right.$$
$$\left. + 2(\mathcal{L}(u^{(n+1)}(x)) - \bar{v}(x)) \frac{\partial \mathcal{L}}{\partial u_i}(u^{(n+1)}(x)) 1_D(x) \right) \varphi_i(x) dx$$
$$= \int_\Omega (w_i^{(n+1)} - w_i^{(n)}) \nabla u_i^{(n+1)}(x) \cdot \nabla \varphi_i(x) dx.$$

For $\frac{1}{q} + \frac{1}{q'} + \frac{1}{2} = 1$, we have

$$\left| \int_\Omega \left(w_i^{(n+1)} \nabla u_i^{(n+1)}(x) \cdot \nabla \varphi_i(x) + 2(u_i^{(n+1)}(x) - \bar{u}_i(x)) 1_{\Omega \setminus D}(x) \right.\right.$$
$$\left.\left. + 2(\mathcal{L}(u^{(n+1)}(x)) - \bar{v}(x)) \frac{\partial \mathcal{L}}{\partial u_i}(u^{(n+1)}(x)) 1_D(x) \right) \varphi_i(x) dx \right|$$
$$\leq \|w_i^{(n+1)} - w_i^{(n)}\|_{L^q} \|\nabla u_i^{(n+1)}\|_{L^{q'}} \|\nabla \varphi_i\|_{L^2}.$$

Since $u^{(n+1)}$ is a minimizer of $\mathcal{E}(u, w^{(n)})$, we may assume without loss of generality that $\hat{u}_i^{(n+1)} = u_i^{(n+1)}$ for all $i = 1, \dots, M$, where $\hat{\cdot}$ is the truncation operator. Consequently $\|u_i^{(n+1)}\|_\infty \leq C < +\infty$ uniformly with respect to n. We can use the results in [28] to show that there exists $q' > 2$ such that

$$\|\nabla u_i^{(n+1)}\|_{L^{q'}} \leq C < +\infty$$

uniformly with respect to n (see also [4, 5, 12] for similar arguments). Therefore, using (7.3), we can conclude that

$$-\operatorname{div}(w_i^{(n+1)} \nabla u_i^{(n+1)}) + 2 \left((u_i^{(n+1)} - \bar{u}_i) 1_{\Omega \setminus D} + (\mathcal{L}(u^{(n+1)}) - \bar{v}) \frac{\partial \mathcal{L}}{\partial u_i}(u^{(n+1)}) 1_D \right) \to 0,$$

for $n \to \infty$, in $(W^{1,2}(\Omega; \mathbb{R}^M))'$. This also shows that $\{u^{(n)}\}_n$ is uniformly bounded in $W^{1,2}(\Omega; \mathbb{R}^M)$. Therefore, there exists a subsequence $\{u^{(n_k)}\}_k$ that converges strongly in L^2 and weakly in $W^{1,2}(\Omega; \mathbb{R}^M)$ to a function $u^{(\infty)} \in W^{1,2}(\Omega; \mathbb{R}^M)$. Since $w_i^{(n+1)} = \frac{\phi_h'(|\nabla u_i^{(n+1)}|)}{|\nabla u_i^{(n+1)}|}$, with standard arguments for monotone operators (see the proof of [12, Proposition 3.1] and [10]), we show that in fact

(7.5)
$$-\operatorname{div}\left(\frac{\phi_h'(|\nabla u_i^{(\infty)}|)}{|\nabla u_i^{(\infty)}|} \nabla u_i^{(\infty)} \right) + 2 \left((u_i^{(\infty)} - \bar{u}_i) 1_{\Omega \setminus D} + (\mathcal{L}(u^{(\infty)}) - \bar{v}) \frac{\partial \mathcal{L}}{\partial u_i}(u^{(\infty)}) 1_D \right) = 0,$$

for $i = 1, \dots, M$, in $(W^{1,2}(\Omega; \mathbb{R}^M))'$. The latter are the Euler–Lagrange equations associated with the functional F_h, and therefore $u^{(\infty)}$ is a stationary point for F_h.

Assume now that F_h has a unique minimizer u^*. Then necessarily $u^{(\infty)} = u^*$. Since every subsequence of $\{u^{(n)}\}_n$ has a subsequence converging to u^*, the full sequence $\{u^{(n)}\}_n$ converges to u^*. ∎

Since both F_h and $\mathcal{E}_h(\cdot, w)$ admit minimizers, their uniqueness is equivalent to the uniqueness of the solutions of the corresponding Euler–Lagrange equations. If uniqueness of the solution is satisfied, then the algorithm (7.2) can be reformulated equivalently as the following two-step iterative procedure:

FIG. 7.1. *The datum* $(\bar{u}, \bar{v})$ *is illustrated in the top-left position. The image has dimensions* 64×78 *pixels. The first four iterations of the algorithms are listed from left to right, starting from the first row. The original color image (A. Mantegna's frescoes, photo by Alinari dated to* 1940*) to be reconstructed is illustrated in the bottom-right position. This image serves as a ground truth for the numerical experiments. The parameters we have used are* $\varepsilon_h = 10^{-4}$, $\lambda = \mu = 150$.

- Find $u^{(n+1)}$, which solves

$$\int_\Omega \Big(w_i^{(n)}(x) \nabla u_i^{(n+1)}(x) \cdot \nabla \varphi_i(x) + 2(u_i^{(n+1)}(x) - \bar{u}_i(x)) 1_{\Omega \setminus D}(x) + 2(\mathcal{L}(u^{(n+1)}(x)) - \bar{v}(x)) \frac{\partial \mathcal{L}}{\partial u_i}(u^{(n+1)}(x)) 1_D(x) \Big) \varphi_i(x) dx = 0$$

  for $i = 1, \ldots, M$ and for all $\varphi \in W^{1,2}(\Omega; \mathbb{R}^M)$.
- Compute directly $w^{(n+1)}$ by

$$w_i^{(n+1)} = \varepsilon_h \vee \frac{1}{|\nabla u_i^{(n+1)}|} \wedge \frac{1}{\varepsilon_h}, \quad i = 1, \ldots, M.$$

There are cases for which one can ensure uniqueness of solutions:

1. If G_2 is strictly convex, then the minimizers are unique as well as the solutions of the equations.

2. Modify the equations by again inserting the parameters $\lambda, \mu > 0$:

$$\int_\Omega \Big(w_i^{(n)} \nabla u_i^{(n+1)}(x) \cdot \nabla \varphi_i(x) + 2\mu (u_i^{(n+1)}(x) - \bar{u}_i(x)) 1_{\Omega \setminus D}(x) + 2\lambda (\mathcal{L}(u^{(n+1)}(x)) - \bar{v}(x)) \frac{\partial \mathcal{L}}{\partial u_i}(u^{(n+1)}(x)) 1_D(x) \Big) \varphi_i(x) dx = 0$$

for $i = 1, \dots, M$ and for all $\varphi \in W^{1,2}(\Omega; \mathbb{R}^M)$. By a standard fixed point argument, it is not difficult to show that for $\mu \sim \lambda \sim \varepsilon_h$ the solution of the previous equations is unique. Unfortunately the condition $\mu \sim \lambda \sim \varepsilon_h$ is acceptable only for those applications where the constraints on the data are weak, for example, when the data are affected by a strong noise.

3. In the following section we illustrate the finite element approximation of the Euler–Lagrange equations. Since we are interested in color image applications, we restrict the numerical experiments to the case $\mathcal{L}(u_1, u_2, u_3) = \frac{1}{3}(u_1 + u_2 + u_3)$. By this choice, the numerical results confirm that the linear systems arising from the finite element discretization are uniquely solvable for a rather large set of possible parameters λ, μ.

8. Numerical implementation and results. In this section we want to present the numerical implementation of the iterative double-minimization algorithm (7.2) for color image restoration. As the second step of the scheme (which amounts to the update of the gradient weight) can be explicitly done once $u^{(n+1)}$ is computed, we are left essentially to provide a numerical implementation of the first step, i.e., the solution of the Euler–Lagrange equations.

8.1. Finite element approximation of the Euler–Lagrange equations. For the solution of the Euler–Lagrange equations we use a finite element approximation. We illustrate the implementation with the concrete aim of the reconstruction of a digital color image supported in $\Omega = [0,1]^2$ from few color fragments supported in $\Omega \setminus D$ and the gray-level information where colors are missing. By the nature of this problem, we can choose a regular triangulation $\mathcal{T}$ of the domain Ω with nodes distributed on a regular grid $\mathcal{N} := \tau \mathbb{Z}^2 \cap \Omega$, corresponding to the pixels of the image. Associated with $\mathcal{T}$ we fix the following finite element spaces:

$$\mathcal{U} = \{u \in C^0(\Omega) : u|T \in \mathbb{P}^1,\ T \in \mathcal{T}\},$$
$$\mathcal{V} = \{w \in L^2(\Omega) : w|T \in \mathbb{P}^0,\ T \in \mathcal{T}\}.$$

The space $\mathcal{U}$ induces the finite element space of color images given by

$$U := \{u \in W^{1,2}(\Omega, \mathbb{R}^3) : u_i \in \mathcal{U},\ i = 1, 2, 3\}.$$

The space $\mathcal{V}$ induces the finite element space of *gradient weights* given by

$$V := \{w \in L^2(\Omega, \mathbb{R}^3) : w_i \in \mathcal{V},\ i = 1, 2, 3\}.$$

In order to avoid the nonlinearity in the coupled terms of order 0, we restrict our functional to the case $\mathcal{L}(u_1, u_2, u_3) = \frac{1}{3}(u_1 + u_2 + u_3)$. For further simplicity we have not considered truncations which in fact are not necessary in practice.

For a given $w^{(n)} \in V$, the first step of our approximation of the double-minimization scheme amounts to the computation of $u^{(n+1)} \in U$, which solves, using (7.4),

$$\int_\Omega \Bigg(w_i^{(n)}(x)\nabla u_i^{(n+1)}(x)\cdot\nabla\varphi_i(x) + 2\mu(u_i^{(n+1)}(x)-\bar u_i(x))1_{\Omega\setminus D}(x) + \frac{2}{3}\lambda\left(\frac{1}{3}(u_1^{(n+1)}(x)+u_2^{(n+1)}(x)+u_3^{(n+1)}(x))-\bar v(x)\right)1_D(x)\Bigg)\varphi_i(x)dx = 0 \tag{8.1}$$

for $i=1,2,3$ and for all $\varphi \in U$. To the spaces $\mathcal{U}$ and $\mathcal{V}$ are attached the corresponding nodal bases $\{\varphi_k\}_{k\in\mathcal{N}}$ and $\{\chi_k\}_{k\in\mathcal{N}}$, respectively. Therefore, we also have that

$$U=\left\{u : u=\left(\sum_{k\in\mathcal{N}} u_{i,k}\varphi_k\right)_{i=1,2,3}\right\},\quad V=\left\{w : w=\left(\sum_{k\in\mathcal{N}} w_{i,k}\chi_k\right)_{i=1,2,3}\right\}.$$

With these bases we can construct the following matrices:

$$\mathbf{K}_i^{(n+1)} := \left(\int_\Omega w_i^{(n)}(x)\nabla\varphi_k(x)\cdot\nabla\varphi_h(x)dx\right)_{k,h\in\mathcal{N}}, \tag{8.2}$$

$$\mathbf{M}_{\Omega\setminus D} := \left(2\mu\int_\Omega 1_{\Omega\setminus D}(x)\varphi_k(x)\varphi_h(x)dx\right)_{k,h\in\mathcal{N}}, \tag{8.3}$$

$$\mathbf{M}_D := \left(\frac{2\lambda}{9}\int_\Omega 1_D(x)\varphi_k(x)\varphi_h(x)dx\right)_{k,h\in\mathcal{N}}. \tag{8.4}$$

By these building blocks, we can assemble

$$\mathbf{K}^{(n+1)} := \begin{pmatrix} \mathbf{K}_1^{(n+1)}+\mathbf{M}_{\Omega\setminus D}+\mathbf{M}_D & \mathbf{M}_D & \mathbf{M}_D \\ \mathbf{M}_D & \mathbf{K}_2^{(n+1)}+\mathbf{M}_{\Omega\setminus D}+\mathbf{M}_D & \mathbf{M}_D \\ \mathbf{M}_D & \mathbf{M}_D & \mathbf{K}_3^{(n+1)}+\mathbf{M}_{\Omega\setminus D}+\mathbf{M}_D \end{pmatrix}$$

and

$$\mathbf{M} := \begin{pmatrix} \mathbf{M}_{\Omega\setminus D}+\mathbf{M}_D & \mathbf{M}_D & \mathbf{M}_D \\ \mathbf{M}_D & \mathbf{M}_{\Omega\setminus D}+\mathbf{M}_D & \mathbf{M}_D \\ \mathbf{M}_D & \mathbf{M}_D & \mathbf{M}_{\Omega\setminus D}+\mathbf{M}_D \end{pmatrix}. \tag{8.5}$$

Furthermore, let us denote the vector of the nodal values of the solution by

$$\mathbf{u}^{(n+1)} = (u_{1,k_1}^{(n+1)},\dots,u_{1,k_{\#\mathcal{N}}}^{(n+1)},u_{2,k_1}^{(n+1)},\dots,u_{2,k_{\#\mathcal{N}}}^{(n+1)},u_{3,k_1}^{(n+1)},\dots,u_{3,k_{\#\mathcal{N}}}^{(n+1)})^T \tag{8.6}$$

assembled as a column vector containing the nodal values of each channel in order, where $k_i \in \mathcal{N}$ are nodes which are suitably ordered. In a similar way the nodal values of the data $\bar u, \bar v$ are assembled in the vector

$$\begin{aligned}\bar{\mathbf{u}} = (&\bar u_{1,k_1},\dots,\bar u_{1,k_j},\bar v_{1,k_{j+1}},\dots,\bar v_{1,k_{\#\mathcal{N}}},\bar u_{2,k_1},\dots,\bar u_{2,k_j},\bar v_{2,k_{j+1}},\dots,\bar v_{2,k_{\#\mathcal{N}}},\\ &\bar u_{3,k_1},\dots,\bar u_{3,k_j},\bar v_{3,k_{j+1}},\dots,\bar v_{3,k_{\#\mathcal{N}}})^T.\end{aligned} \tag{8.7}$$

For the right-hand side we have the additional requirement that $\bar v_{i,k} = \bar v_{\ell,k}$ for $i \neq \ell$, representing the gray-level values. Moreover, the order of the nodes $\{k_l : l=1,\dots,\#\mathcal{N}\}$ is such that

$$(\mathbf{M}_{\Omega\setminus D}+\mathbf{M}_D)(\bar u_{i,k_1},\dots,\bar u_{i,k_j},\bar v_{i,k_{j+1}},\dots,\bar v_{i,k_{\#\mathcal{N}}})^T = \mathbf{M}_{\Omega\setminus D}\begin{pmatrix}\bar{\mathbf{u}}_\mathbf{i}\\0\end{pmatrix}+\mathbf{M}_D\begin{pmatrix}0\\\bar{\mathbf{v}}_\mathbf{i}\end{pmatrix}.$$

With these notations and conventions, the solution of the system of equations (8.1) is equivalent to the solution of the following algebraic linear system:

$$\mathbf{K}^{(n+1)}\mathbf{u}^{(n+1)} = \mathbf{M}\bar{\mathbf{u}}. \tag{8.8}$$

8.2. Numerical implementation of the double-minimization algorithm. We have now all the ingredients to assemble our numerical scheme into the following algorithm.

ALGORITHM 1. **DOUBLE_MINIMIZATION**

Input: Data vector $\bar{\mathbf{u}}$, $\varepsilon_h > 0$, initial gradient weight $w^{(0)}$ with $\varepsilon_h \le w_{i,k}^{(0)} \le 1/\varepsilon_h$, number $n_{\max}$ of outer iterations.

Parameters: Positive weights $\lambda, \mu \ge 0$.

Output: Approximation u^* of the minimizer of F_h

$\mathbf{u}^{(0)} := 0$;

$\mathbf{f} := \mathbf{M}\bar{\mathbf{u}}$;

for $n := 0$ *to* $n_{\max}$ *do*

Assemble the matrix $\mathbf{K}^{(n+1)}$ as in (8.2);

Compute $\mathbf{u}^{(n+1)}$ such that $\mathbf{K}^{(n+1)}\mathbf{u}^{(n+1)} := \mathbf{f}$;

Assemble the solution $u^{(n+1)} = (\sum_{k\in\mathcal{N}} u_{i,k}^{(n+1)}\varphi_k)_{i=1,2,3}$;

Compute the gradient $\nabla u^{(n+1)} = (\sum_{k\in\mathcal{N}} u_{i,k}^{(n+1)}\nabla\varphi_k)_{i=1,2,3}$;

$w_i^{(n+1)} := \varepsilon_h \vee \frac{1}{|\nabla u_i^{(n+1)}|} \wedge \frac{1}{\varepsilon_h}, \quad i = 1, \dots, M;$

endfor

$u^* := u^{(n+1)}$.

8.3. Numerical experiments in color image restoration and results. In this section we show numerical results dealing with applications of the algorithm to color image restoration. We assume as in Figure 1.1 to have available few color fragments of the image and the gray levels of the missing parts. In all the experiments we report, we also furnish a corresponding ground truth image for comparison. The support of the image is $\Omega = [0,1]^2$, where we construct a grid of dimensions $h \times w$, and w and h are the width and height of the image in pixels, respectively. On this grid a regular triangulation is defined. The values of the images are in $[0, 255]$ channelwise.

The algorithm converges to a stationary situation in a limited number of iterations. In our numerical tests 3–4 iterations are sufficient; see Figures 7.1 and 8.4. The quality of the reconstruction increases for increasing the amount of correct color information of the datum. Nevertheless we observe that the geometrical distribution of the color datum is more crucial for a better reconstruction. A remarkable result is illustrated in Figures 8.1 and 8.2. In the bottom-left positions we illustrate data with only 3% of the original color information, randomly distributed. From this very limited complete information the algorithm still produces a rather good reconstruction of the original color images. Let us emphasize this once more:

It is sufficient to have a very limited guess of possible colors which are nicely distributed in the image to recolor all of the image.

This result has a significant impact for several possible applications. Besides the problem of the restoration of the fresco colors (where we have available 8% of the total color surface), we can use this algorithm in old black and white video and image restoration and for extreme compression of color images. For the sake of further reference, in Figure 8.3 we illustrate a comparison between the algorithm proposed in [26] and our reconstruction. In our experiments the results appear visually equivalent, although our method tends to reproduce more accurately the luminosity of the image,

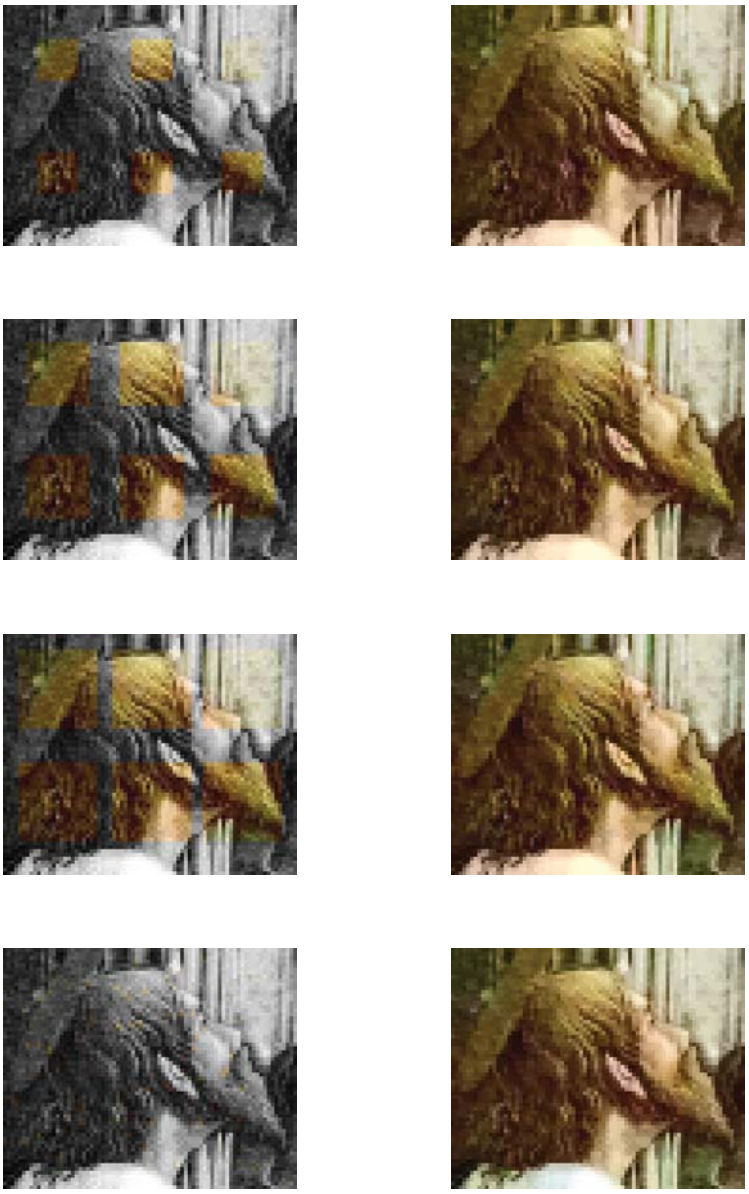

FIG. 8.1. *The first column illustrates a sequence of different data. The second column illustrates the corresponding* 10*th iteration of the algorithm. The original color image to be reconstructed is illustrated in Figure* 7.1 *in the bottom-right position. The parameters we have used are* $\varepsilon_h = 10^{-4}$, $\lambda = \mu = 150$. *In the bottom-left position we illustrate a datum with only* 3% *of the original color information, randomly distributed.*

because of the enforced constraint of the gray-level reproduction in the inpainting region. The method proposed in [26] can perform slightly better pick signal-to-noise ratios (PSNRs), though in most of the cases they do not differ significantly. For a more specific discussion on fidelity in recolorization, we refer the reader to [22]. We

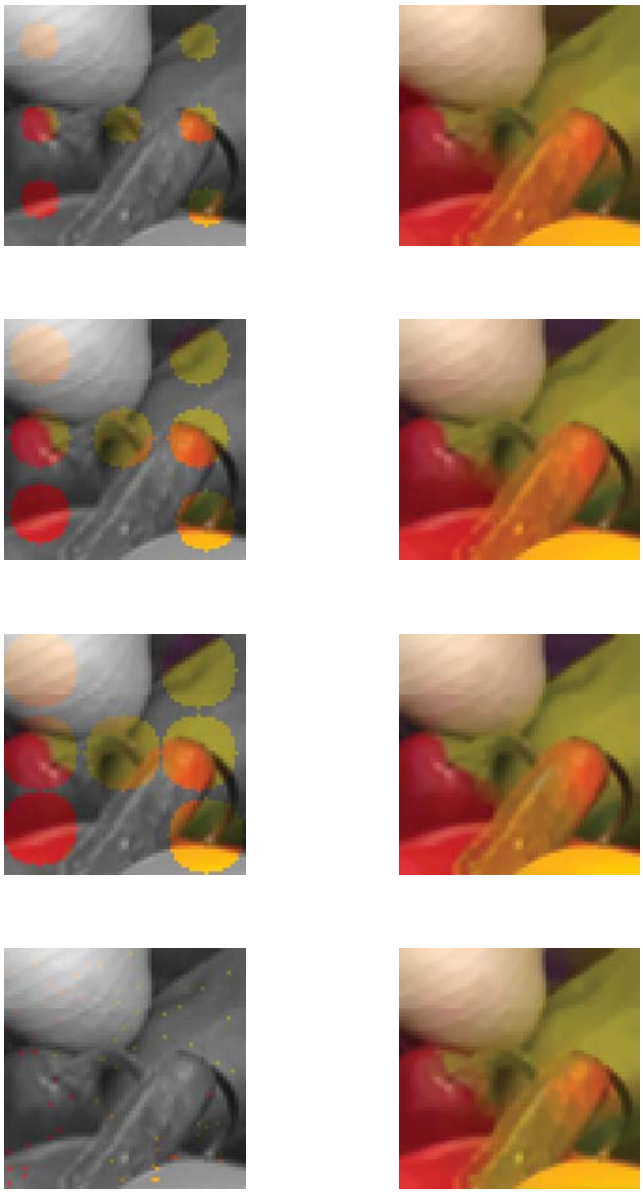

FIG. 8.2. *The first column illustrates a sequence of different data. The second column illustrates the corresponding* 10*th iteration of the algorithm. The parameters we have used are* $\varepsilon_h = 10^{-4}$, $\lambda = \mu = 150$. *In the bottom-left position we illustrate a datum with only* 3% *of the original color information, randomly distributed. The original color image to be reconstructed is illustrated in the top-right position of Figure* 8.3. *This image serves as a ground truth for the numerical experiments.*

conclude with a brief discussion on the parameters $\lambda, \mu, \varepsilon_h$. In Figure 8.4 we show the history of the residual error with respect to the original color image for increasing choices of the parameters λ, μ. These numerical results confirm the regularization effect due to the total variation constraint. The choice of ε_h has a twofold function. It

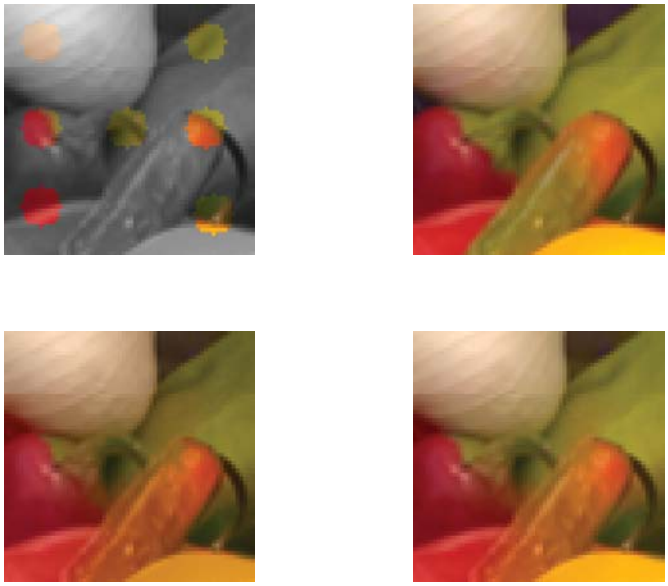

FIG. 8.3. *The figure on the top-left reports the initial data, and on the top-right we have the original image. The figure on the bottom-left is the recolorization by means of the algorithm presented in* [26] *generated by the MATLAB code provided at http://www.cs.huji.ac.il/∼yweiss/Colorization/colorization.zip. On the bottom-right we again report the reconstruction due to our algorithm. The PSNR of a color image u with respect to a ground truth image $\bar{u}$ is defined by* $PSNR = 10\log_{10}\left(\frac{255^2}{\frac{1}{3hw}\sum_{i=1}^{3}\|u_i-\bar{u}_i\|_2^2}\right)$, *where h, w are the height and width of the image, respectively. Although the PSNRs are* 31.61 *dB and* 29.48 *dB, respectively, particularly visible is a more accurate luminosity restoration, e.g., in the yellow region, due to our algorithm.*

serves as a regularization parameter; i.e., the visual smoothness of the reconstruction depends on ε_h. The larger values of ε_h give smoother reconstructed images. This effect is due to the fact that if ε_h gets large, then the corresponding differential operator $\nabla\cdot\left(\frac{\phi_h'(|\nabla u_i|)}{|\nabla u_i|}\nabla u_i\right)$ becomes more and more isotropic. Moreover, since in discrete images the gradients are always bounded, if ε_h is smaller than a threshold $T>0$ depending on the mesh size τ—in our experiments $T=(255\max\{h,w\})^{-1}$—then the lower bound on the gradient weight becomes irrelevant in the algorithm. However, the second purpose of this parameter is also for the sake of numerical stability. Depending on the size of the image, this parameter cannot be too small (i.e., minimal); otherwise the corresponding stiffness matrices $\mathbf{K}^{(n)}$ might be significantly ill-conditioned, and suitable preconditioners (multigrid and subspace correction/domain decomposition methods) should be invoked in this case.

Acknowledgments. The first author acknowledges the hospitality of NuHAG (the Numerical Harmonic Analysis Group), Faculty of Mathematics, University of Vienna, during the early preparation of this work. The second author wishes to thank Prof. N. Fusco for a helpful discussion. Both authors would like to thank the anonymous referees for their useful comments and suggestions.

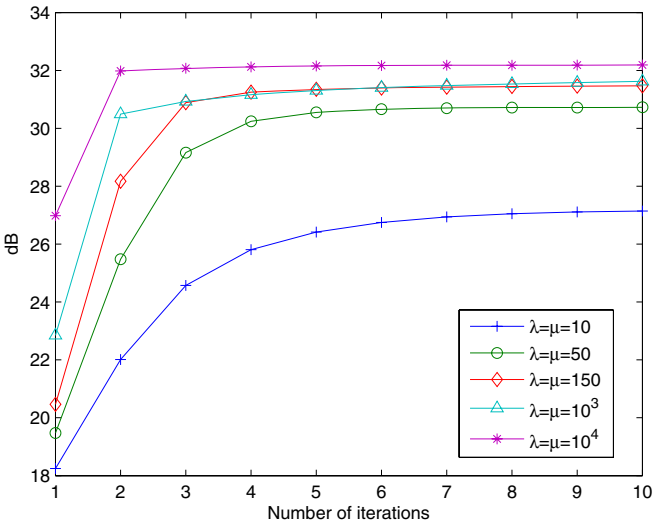

FIG. 8.4. *The plots illustrate the PSNR for different iterations of the algorithm applied to the image in Figure* 7.1 *and for different values of the parameters* λ, μ.

REFERENCES

[1] L. AMBROSIO, *A compactness theorem for a new class of functions of bounded variation*, Boll. Un. Mat. Ital. B (7), 3 (1989), pp. 857–881.

[2] L. AMBROSIO, N. FUSCO, AND D. PALLARA, *Functions of Bounded Variation and Free Discontinuity Problems*, Oxford Math. Monogr., Clarendon Press, Oxford University Press, New York, 2000.

[3] L. AMBROSIO AND S. MASNOU, *A direct variational approach to a problem arising in image reconstruction*, Interfaces Free Bound., 5 (2003), pp. 63–81.

[4] G. AUBERT, R. DERICHE, AND P. KORNPROBST, *Computing optical flow via variational techniques*, SIAM J. Appl. Math., 60 (1999), pp. 156–182.

[5] G. AUBERT AND P. KORNPROBST, *A mathematical study of the relaxed optical flow problem in the space* $BV(\Omega)$, SIAM J. Math. Anal., 30 (1999), pp. 1282–1308.

[6] G. AUBERT AND P. KORNPROBST, *Mathematical Problems in Image Processing. Partial Differential Equations and the Calculus of Variations*, Springer-Verlag, New York, 2002.

[7] G. AUBERT AND L. VESE, *A variational method in image recovery*, SIAM J. Numer. Anal., 34 (1997), pp. 1948–1979.

[8] C. BALLESTER, M. BERTALMIO, V. CASELLES, G. SAPIRO, AND J. VERDERA, *Filling-in by joint interpolation of vector fields and gray levels*, IEEE Trans. Image Process., 10 (2001), pp. 1200–1211.

[9] M. BELTRAMIO, G. SAPIRO, V. CASELLES, AND B. BALLESTER, *Image inpainting*, in Proceedings of the 27th Annual ACM Conference on Computer Graphics, 2000, pp. 417–424.

[10] H. BRÉZIS, *Opérateurs maximaux monotones et semi-groupes de contractions dans les espaces de Hilbert*, North–Holland Math. Stud. 5, North–Holland, Amsterdam, London, American Elsevier, New York, 1973.

[11] A. BROOK, R. KIMMEL, AND N. A. SOCHEN, *Variational restoration and edge detection for color images*, J. Math. Imaging Vision, 18 (2003), pp. 247–268.

[12] A. CHAMBOLLE AND P.-L. LIONS, *Image recovery via total variation minimization and related problems*, Numer. Math., 76 (1997), pp. 167–188.

[13] T. F. CHAN, S. H. KANG, AND J. SHEN, *Euler's elastica and curvature-based inpainting*, SIAM J. Appl. Math., 63 (2002), pp. 564–592.

[14] T. F. CHAN AND J. SHEN, *Inpainting based on nonlinear transport and diffusion*, in Inverse Problems, Image Analysis, and Medical Imaging, Contemp. Math. 313, AMS, Providence, RI, 2002, pp. 53–65.

[15] T. F. Chan and J. Shen, *Mathematical models for local nontexture inpaintings*, SIAM J. Appl. Math., 62 (2002), pp. 1019–1043.
[16] T. F. Chan and J. Shen, *Variational image inpainting*, Comm. Pure Appl. Math., 58 (2005), pp. 579–619.
[17] D. Demengel and R. Temam, *Convex functions of a measure and applications*, Indiana Univ. Math. J., 33 (1984), pp. 673–709.
[18] D. C. Dobson and C. R. Vogel, *Convergence of an iterative method for total variation denoising*, SIAM J. Numer. Anal., 34 (1997), pp. 1779–1791.
[19] I. Ekeland and R. Temam, *Convex Analysis and Variational Problems*, Stud. Math. Appl. 1, North–Holland, Amsterdam, Oxford, American Elsevier, New York, 1976; reprinted, SIAM, Philadelphia, 1999.
[20] L. C. Evans and R. F. Gariepy, *Measure Theory and Fine Properties of Functions*, CRC Press, Boca Raton, FL, 1992.
[21] M. Fornasier, *Nonlinear projection recovery in digital inpainting for color image restoration*, J. Math. Imaging Vision, 24 (2006), pp. 359–373.
[22] M. Fornasier, *Faithful recovery of vector valued functions from incomplete data. Recolorization and art restoration*, in Proceedings of the First International Conference on Scale Space and Variational Methods in Computer Vision, Lecture Notes in Comput. Sci. 4485, F. Sgallari, A. Murli, and N. Paragios, eds., Springer-Verlag, Berlin, 2007, pp. 116–127.
[23] M. Fornasier and H. Rauhut, *Recovery algorithms for vector valued data with joint sparsity constraints*, SIAM J. Numer. Anal., to appear.
[24] M. Fornasier and D. Toniolo, *Fast, robust and efficient* $2D$ *pattern recognition for reassembling fragmented images*, Pattern Recognition, 38 (2005), pp. 2074–2087.
[25] C. Goffman and P. A. Raviart, *Sublinear functions of measures and variational integrals*, Duke Math. J., 31 (1964), pp. 159–178.
[26] A. Levin, D. Lischinski, and Y. Weiss, *Colorization using optimization*, ACM Trans. Graph., 23 (2004), pp. 689–694.
[27] G. Dal Maso, *An Introduction to* Γ*-Convergence*, Birkhäuser, Boston, 1993.
[28] N. Meyers, *An* L^p*-estimate for the gradient of solutions of second order elliptic divergence equations*, Ann. Scuola Norm. Sup. Pisa (3), 17 (1963), pp. 189–206.
[29] D. Mumford and J. Shah, *Optimal approximation by piecewise smooth functions and associated variational problems*, Comm. Pure Appl. Math., 42 (1989), pp. 577–684.
[30] L. I. Rudin, S. Osher, and E. Fatemi, *Nonlinear total variation based noise removal algorithms*, Phys. D, 60 (1992), pp. 259–268.
[31] L. Vese, *A study in the* BV *space of a denoising-deblurring variational problem*, Appl. Math. Optim., 44 (2001), pp. 131–161.
[32] C. R. Vogel and M. E. Oman, *Iterative methods for total variation denoising*, SIAM J. Sci. Comput., 17 (1996), pp. 227–238.
[33] L. Yatziv and G. Sapiro, *Fast image and video colorization using chrominance blending*, IEEE Trans. Image Process., 15 (2006), pp. 1120–1129.